Journal of Colloid and Interface Science 607 (2022) 389–400

Contents lists available at ScienceDirect

Journal of Colloid and Interface Science

journal homepage: www.elsevier.com/locate/jcis

Rheological behaviour of attractive emulsions differing in droplet-droplet interaction strength

Philipp L. Fuhrmann [a,b], Swantje Breunig [b], Guido Sala [b], Leonard Sagis [b], Markus Stieger [a,c,d], Elke Scholten [a,b,*]

[a] TiFN, P.O. Box 557, 6700 AN Wageningen, the Netherlands
[b] Physics and Physical Chemistry of Foods, Wageningen University & Research, P.O. Box 17, 6700 AA Wageningen, the Netherlands
[c] Division of Human Nutrition and Health, Wageningen University & Research, P.O. Box 17, 6700 AA Wageningen, the Netherlands
[d] Food Quality and Design Group, Wageningen University & Research, P.O. Box 17, 6700 AA Wageningen, the Netherlands

HIGHLIGHTS

- Droplet interactions tune emulsion rheology from soft-solid to glassy- to gel-like
- LAOS rheology mapped over broad range of droplet-droplet interactions
- Current system of emulsion rheology characterisation might not be sufficient

GRAPHICAL ABSTRACT

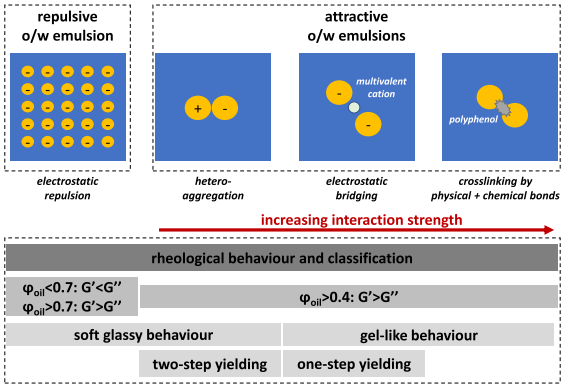

ARTICLE INFO

Article history:
Received 29 December 2020
Revised 17 August 2021
Accepted 18 August 2021
Available online 25 August 2021

Keywords:
Emulsion
Rheology
Yielding
LAOS
Droplet-droplet interaction
Polyphenol
Clustering

ABSTRACT

Hypothesis: We hypothesise that interaction strength between oil droplets determine the rheological properties of oil-in-water (O/W) emulsions by simultaneous formation and break-up of bonds between droplets. Using small (SAOS) and large (LAOS) amplitude oscillatory shear measurements, we aim to distinguish different classes of emulsions based on the specific microstructural evolution of the emulsions.
Experiments: Concentrated O/W emulsions differing in droplet-droplet interaction strength were obtained. Different interaction strength was obtained using different types of interactions; (a) electrostatic attraction, (b) salt bridging, or (c) crosslinking.
Findings: In line with our hypothesis, different rheological events in emulsions depend on the droplet-droplet interaction strength. Strong interactions lead to monotonous yielding, and droplets undergo jamming or densification to provide strain hardening and gel-like behaviour. Emulsions with weak interactions exhibit two-step yielding (SAOS) and continuous yielding in LAOS; indicating a soft-glassy material. In emulsions above maximum packing, and with weak interactions the rheology is controlled by cluster/cage breaking, and transient formation of new clusters. For medium-strength interactions, two-step yielding was reduced, and apparent stain-hardening occurred. The probability of two distinct time scales

* Corresponding author at: Physics and Physical Chemistry of Foods, Wageningen University & Research, P.O. Box 17, 6700 AA Wageningen, the Netherlands.
E-mail address: elke.scholten@wur.nl (E. Scholten).

https://doi.org/10.1016/j.jcis.2021.08.124

of yielding is hindered by stronger interactions and jamming. Overall, in concentrated emulsions, yielding is determined by network rupture and reformation, cluster rearrangement and -breaking, which in turn is influenced by interaction type and strength. We present a more differentiated categorisation of emulsions based on interaction strength.

1. Introduction

Oil-in-water emulsions are ubiquitous materials [1]. Their rheological behaviour is influenced by their composition, microstructure, and their interactions [2]. At low volume fractions ($\phi < 0.1$) of oil droplets, emulsions behave as Newtonian liquids. When the oil fraction increases ($\phi > 0.1$), droplet-droplet contact occurs, and emulsions show non-Newtonian flow behaviour. With further increasing volume fraction, the shear viscosity increases due to the dense packing of the droplets. As the oil droplets approach maximum packing ($\phi_{max,}$ 0.64 for random close packing or 0.74 for hexagonal close packing of monodisperse droplets), the system is still in a liquid state, but beyond this packing fraction, the emulsion becomes a soft solid and displays yielding behaviour. When droplets are deformable (i.e., when their Laplace pressure is relatively low), the oil volume fraction can be increased above the maximum packing fraction. In this case, the emulsion starts to show viscoelastic solid properties, with a strong dependence of the elasticity on interfacial properties. In the case of interactions between the droplets, the maximum packing fraction can deviate from its hard-sphere value. In repulsive emulsions, i.e. emulsions with repulsive droplet interactions [3], the maximum packing fraction decreases as the droplets start to repel each other, thereby increasing their effective size [4]. In the case of attractive interactions, the maximum packing fraction also decreases, as oil droplets start to cluster, leading to network formation already at lower volume fractions. As a result, the effective oil volume fraction is considerably increased, and the emulsions display elastic properties at volume fractions below random close packing [5]. For repulsive emulsions, an increase in oil volume fraction leads to a rheological behaviour where the elastic modulus (G′) dominates over the viscous modulus (G″), indicating predominantly elastic behaviour. With increasing shear strain, both moduli decrease due to network breakage and droplet alignment, and predominantly viscous behaviour prevails. In the case of concentrated emulsions with purely repulsive interactions, the viscous modulus can exhibit a peak at a specific strain value [6], which is related to the temporary jamming and the subsequent structural relaxation of the oil droplets [7].

When emulsion droplets experience attractive interactions, referred to as attractive emulsions, clustering of droplets occurs [8]. In some cases, a two-step yielding behaviour of G″, visible as two peaks, has been described [6]. Similar behaviour was shown for microgel particle suspensions [7,9]. It was suggested that this two-step yielding relates to the occurrence of two rearrangement phenomena. In the first yielding process, interactions and bonds between particles are assumed to be disturbed. The first peak thus relates to the initial breakdown of inter-particle interactions. Although fewer interactions are then present between the particles, particles are still immobilised. In the second yielding step, a temporary stiffening by particle rearrangement occurs, followed by a collapse of the structure. Thus, the occurrence of a two-step yielding phenomenon is linked, in literature, to the co-existence of two different time scales or structural relaxation processes and two specific length scales – particle-particle interactions and cage characteristics [10]. Studies on microgel particle dispersions have shown that the two-step yielding process only occurs in a limited range of volume fractions of attractive particles [9,10]. At volume fractions below this range, no yielding behaviour was observed, and at higher volume fractions one-step yielding behaviour was found. In most of these previous studies, attractive interactions are induced by depletion interactions, which leads to weak indirect attractive interactions. In addition, most studies have been performed with suspensions. Two important factors remain unclear; firstly, what is the role of interaction strength between droplets on the yielding behaviour of O/W emulsions, and secondly, what is the effect of those droplet-droplet interactions on large deformation rheological properties (LAOS). By including LAOS measurements, the specific non-linear behaviour can provide additional information on structural changes within the emulsions. This study aimed to investigate the effect of droplet-droplet interactions in emulsions with high oil volume fractions on the rheological behaviour both at small and large deformations. In this study, we use direct attractive interactions to change the interaction strength. We varied the droplet-droplet interactions by using different types of interactions: (i) electrostatic attraction, (ii) salt bridging and (iii) crosslinking of protein-stabilised oil droplets with polyphenolic compounds. As the strength of droplet-droplet interactions is a result of the type of the interactions and environmental conditions (such as pH), we use emulsions since the interfacial composition can be easily changed. To characterise the emulsions, oscillatory shear rheology measurements at small- and large-amplitudes were performed. Large deformation tests probe events in the non-linear regime and can provide additional insights on the structural organization of the systems. Next to microstructural visualization of materials under flow and light scattering techniques, this leads to easily accessible complementary information.

2. Experimental

2.1. Materials

Whey protein isolate (WPI, BiPRO) was obtained from Davisco (Le Sueur, MN, USA). Gelatine (type A) was acquired from Rousselot (Son, The Netherlands). Diacetyl tartaric acid ester of mono- and diglycerides (DATEM) was kindly provided by CP Kelco Inc (Atlanta, GA, USA). As a source of polyphenols, grape seed extract ("GSE", Vitaflavan®) produced by Les Dérivés Résiniques et Terpéniques (Dax, France) was used. Sunflower oil was obtained from a local supermarket. $CaCl_2$, HCl, NaOH, citric acid and disodium hydrogen phosphate were obtained from Sigma Aldrich (St. Louis, USA). For all experiments, demineralised water was used (MilliQ® system, Merck Millipore, Germany).

2.2. Methods

2.2.1. Preparation of O/W emulsions

2.2.1.1. O/W emulsions with repulsive droplet-droplet interactions. To obtain O/W emulsions with 40% (v/v) oil, an aqueous phase containing 7.5 g/L WPI in water was prepared. The mixture was stirred overnight at 4 °C, and the pH was adjusted (6.8, 1 M HCl/NaOH). After addition of the oil phase, the mixture was pre-emulsified with a rotor–stator homogeniser (Ultra-Turrax, IKA, Germany) at

8000 rpm for 3 min. The pre-emulsions were homogenised four times (LabhoScope, Delta Instruments, The Netherlands) at 180 bars. Emulsions with higher oil volume fractions were obtained by centrifugation as described in Section 2.2.1.3.

2.2.1.2. Preparation of O/W emulsions with attractive droplet-droplet interactions.

Emulsions with weak attractive interactions: Hetero-aggregated O/W emulsions. O/W emulsions with 40% (v/v) oil and with hetero-aggregated clusters were prepared by combining a WPI-stabilised and a gelatine-stabilised emulsion. O/W emulsions with gelatine were made by preparing an aqueous phase containing 9.6 g/L gelatine in water. The gelatine dispersion was heated in a water bath at 80 °C for 30 min. At room temperature, the pH was set to pH 5 (1 M HCl/NaOH). After the addition of the oil phase (40%(v/v)), the mixture was pre-emulsified and homogenised as described earlier. O/W emulsions with WPI were prepared by dissolving WPI (6.4 g/L) in an aqueous phase. After addition of the oil phase, the mixture was pre-emulsified with a rotor–stator homogeniser (Ultra-Turrax, IKA, Germany) at 8000 rpm for 3 min. The pre-emulsions were homogenised four times (LabhoScope, Delta Instruments, The Netherlands) at 180 bars. The emulsions were stored at room temperature for 24 h. Hetero-aggregated emulsions were obtained by combining the two emulsions at a volumetric ratio of 1:1, at pH 5. After mixing, the emulsions were stored for 24 h before further use. Emulsions with higher oil volume fractions were obtained by centrifugation of the emulsions as described in Section 2.2.1.3.

Emulsions with medium-strength attractive interactions: Salt bridged O/W emulsions. A WPI-stabilised emulsion (7.5 g/L) with 40%(v/v) oil was prepared as described in Section 2.2.1.1. An aqueous solution of $CaCl_2{\cdot}2H_2O$ (0.74 g/mL) was prepared and added to the emulsions to obtain final salt concentrations between 0.01 and 0.26 mol/L to create salt bridging. Samples were mixed and stored for 30 min before further use. Emulsions with higher oil volume fractions were obtained by centrifugation (Section 2.2.1.3). Interactions between the oil droplets were already induced before concentrating the emulsions.

Emulsions with strong attractive interactions ("cross-linked emulsions"): WPI-stabilised O/W emulsions with polyphenol-induced clustering.. For the aqueous phase, WPI (7.5 g/L) was dissolved in a 0.12 M McIlvaine buffer at pH 3 overnight. The pH was adjusted with 1 M HCl when required. Sunflower oil (40% v/v) was added to the aqueous phase. The emulsion was pre-homogenised and homogenised as described before. After homogenisation, 0.75 g grape seed extract (GSE) per gram of emulsifying protein was added as an aqueous stock solution of GSE of 200 g/L in pH 3 McIlvaine buffer as described before [8]. Dilution due to the addition of this solution was considered negligible. After addition of the GSE solution, the emulsions were shaken and stored at room temperature for 24 h before further use [8]. During storage, the GSE induced strong interactions between the oil droplets by binding to the proteins present at the oil droplet interface; these interactions include strong physical interactions, but covalent interactions may also be present [8]. Emulsions with higher oil volume fractions were obtained as described before.

The interaction strength between emulsion droplets was estimated based on our earlier work, where we use the critical strain as an indication of aggregation strength [8]. Hetero-aggregates (electrostatic interaction) are indeed formed through weaker interactions than the aggregates formed by polyphenols (GSE) (critical strain of hetero-aggregated emulsions of about 1.8% and polyphenol-aggregated emulsions about 6%, both at an oil volume fraction of 0.2). Due to the weaker interactions, we consider hetero-aggregated emulsions as reversibly bound, and droplets can therefore rearrange within the time scale of the experiments. The stronger physical interactions and potential covalent interactions of the polyphenol-aggregated emulsions lead to irreversibly bound droplets, and therefore rearrangements are less likely to occur within the time frame of the experiments. Emulsions with salt bridges (Ca^{2+}) show critical strains between those of hetero-aggregated emulsions and emulsions with chemical crosslinking (polyphenols). We classify these interactions as "medium-strength attractive interactions" and are considered reversible. The interaction strength thus indeed varied with the type of interaction and the environmental conditions used.

2.2.1.3. Increase in oil volume fraction of the emulsions. To achieve higher oil volume fractions, emulsions were concentrated by centrifugation (Beckmann, Avanti J-26 XP, Beckman Coulter B.V., Mijdrecht, The Netherlands) for 30 min at 20.000 rpm and subsequently diluted with the corresponding aqueous phase (without emulsifier). Droplet size was determined using static light scattering (Mastersizer 2000S, Malvern Instruments, Ltd., Worcester, UK), and a refractive index of 1.47 and 1.33 was used for the dispersed and continuous phase, respectively. The droplet size did not differ before and after centrifugation, indicating that only limited coalescence of the emulsion droplets took place.

2.2.2. Physical characterisation of O/W emulsions

2.2.2.1. Rheological characterisation. Rheological measurements were conducted with an Anton Paar 302 Rheometer (MCR 302, Anton Paar GmbH, Austria). A parallel plate geometry (PP25) was used. The gap size was set to 0.5 mm. We used serrated plates to avoid wall-slip. After loading the samples, a resting time of 1 min was used to allow structural relaxation of the sample before starting the measurement. Low viscous paraffin oil was added at the edges of the geometry to avoid evaporation of the water in the samples during measurements.

2.2.2.2. Small amplitude oscillatory shear (SAOS). SAOS measurements were used to determine the viscoelastic properties of the emulsions at small deformation, i.e., in the linear viscoelastic regime. To determine G′ and G″, an amplitude sweep was performed with a shear strain range of 0.01–1000%, with a logarithmic ramp. The test was performed at a frequency of 10/s at 20 °C. Frequency sweeps at a strain within the linear range showed that the moduli were nearly frequency independent in the applied frequency range and showed weak power-law behaviour: $G' \sim \omega^n$, with n close to zero. An example of a frequency sweep of a repulsive emulsion can be found in the supplementary data (S1). We determined the elastic modulus G′, the viscous modulus G", the critical strain, and the cross-over point of G′ and G". We defined the critical strain as the strain at which the elastic modulus shows a clear decrease, in this case, taken as a 10% deviation in the modulus. We identify the yield strain of the material in the amplitude sweep as the occurrence of a sudden change in slope of the modulus as a function of strain, as described in earlier research [11]. In some cases, also a two-step yielding can be identified, which can be recognised by the occurrence of two changes in the slope throughout the amplitude range.

2.2.2.3. Large amplitude oscillatory shear (LAOS). The elastic and viscous response of the emulsions in the non-linear regime was determined by large deformation, i.e., LAOS measurements. The amplitude was varied in the range of 0.01–1000% at a constant frequency of 10/s at 20 °C. Lissajous-Bowditch plots were created to describe the response of the emulsions. Following an earlier published approach, we show Lissajous-Bowditch plots in 4 regimes based on the variation of G′ and G″ with strain amplitude [9]. These regimes include: (i) a strain range in the linear regime of G′/G″, (ii) at the yield points, (iii) at the maximum of G", and (iv) at high strains. A schematic display of these regimes can be found in the

supplementary data S2. The intra-cycle strain stiffening behaviour (S factor) and intra-cycle shear thickening behaviour (T factor) were determined as described in literature [12,13], following

$$S = \frac{G'_L - G'_M}{G'_L} \quad (1)$$

And

$$T = \frac{\eta'_L - \eta'_M}{\eta'_L} \quad (2)$$

where G'_L and G'_M are the large-strain and minimum-strain elastic modulus, respectively. η'_L and η'_M are the large-rate and minimum-rate dynamic viscosity, respectively.

Those factors are dimensionless numbers, which can be used to identify strain stiffening (S > 0) or strain softening (S < 0) behaviour, and shear thickening (T > 0) or shear thinning (T < 0) behaviour [14].

2.2.2.4. Determination of oil volume fraction. The oil volume fraction of samples was estimated by determining the dry matter content of concentrated emulsions. Emulsions were dried for 24 h at 120 °C (Binder Oven, Binder GmbH, Tuttlingen, Germany) and dry matter was subsequently gravimetrically determined correcting for added emulsifier. All samples were measured in triplicates.

2.2.2.5. Zeta potential. The ζ-potential of gelatine and WPI-stabilised emulsions was determined using a Zetasizer Nano ZS series (Malvern Instruments, Worcestershire, UK). Non-clustered emulsions were diluted 100 times with the emulsifier-free aqueous phase (MiliQ water). Samples were measured in triplicates at 20 °C.

3. Results and discussion

3.1. Emulsion rheology

3.1.1. Repulsive emulsions

WPI-stabilised O/W-emulsions (pH 6.8, zeta potential = −38 m V) were used as reference repulsive emulsions. The large net negative charge of the proteins was sufficient to prevent aggregation. For all samples (ϕ of 0.7–0.85), G′ was initially higher than G″, revealing a solid-like nature of the emulsions at low strains. The graph can be found in the supplementary data (S3). The solid-like, elastic behaviour can be observed in the Lissajous-Bowditch plots (Fig. 1A), as the curve has a narrow elliptic shape at a small strain (Fig. 1). The individual loops shifted over time slightly downward in their stress response. The reason for this is that at low strains and torque values, oscillations tend to take a longer time to reach a steady-state. G′ increases in a repulsive emulsion with increasing ϕ, as the emulsion droplets contribute to the elasticity of the network. In the Lissajous-Bowditch plots, the onset of non-linearity could be observed as a widening of the elliptic curve (Fig. 1B and C). With increasing strain, emulsion behaved, therefore, as a repulsive soft glass, which has also been shown in the work of others [15]. G′ increased by more than two orders of magnitude as ϕ increased from 0.70 to 0.85. Just beyond the critical strain, G′ decreased as γ increased, but G″ first showed a local maximum at intermediate strain values (γ = 20–50%) before it decreased, i.e., we observe a weak strain overshoot. This behaviour is referred to as a so-called type III behaviour, as suggested by Hyun and coworkers [16,36]. The overall strain-softening behaviour of the emulsion can be observed in the Lissajous-Bowditch plot at higher strain (Fig. 1C and D), where the curve shows a more rhomboidal shape. In the *T*-factor, defined as thickening factor, we observe a local maximum (Fig. 1), which indicates intra-cycle shear rate thickening behaviour, followed by shear thinning. Due to the G″ overshoot and the maximum in the stiffening ratio, we can assume that an initial network structure was present and that the emulsions did not suddenly collapse [17]. Although we do not have direct proof of dynamic changes in the network structure, typical events have been discussed in literature already [18]. The rheological behaviour suggests that the emulsion droplets in such a repulsive network are held together quasi in a cage at high volume fractions. At high strains, the droplets become mobile after escaping the cage, also referred to as cage breaking [7,19]. With increasing ϕ, it is more difficult for droplets to become mobile and escape from the cage and allow the emulsion to flow, thus the overshoot in G″ increases with droplet volume fraction. This behaviour has

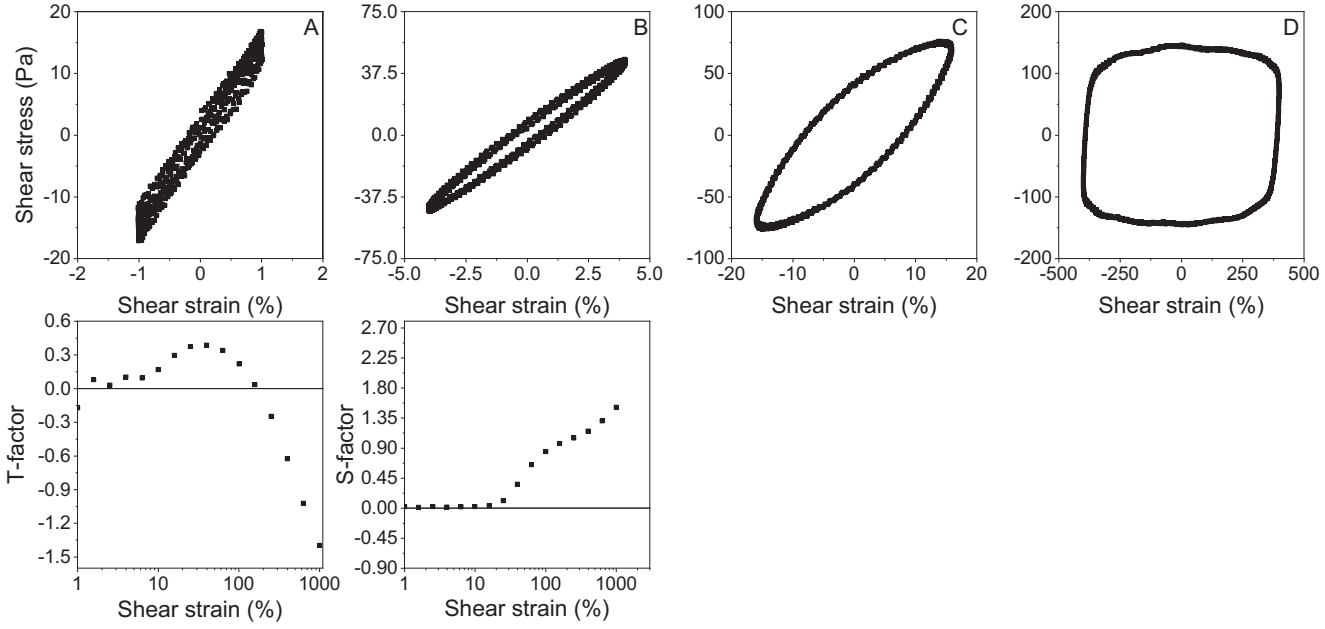

Fig. 1. Overview of LAOS measurements (shear strain vs stress) in 4 strain regions of a repulsive emulsion (0.8 oil), the strains in question are: 1% (A), 4% (B), 16% (C) and 400% (D). S- and *T*-factors are shown as a function of shear strain.

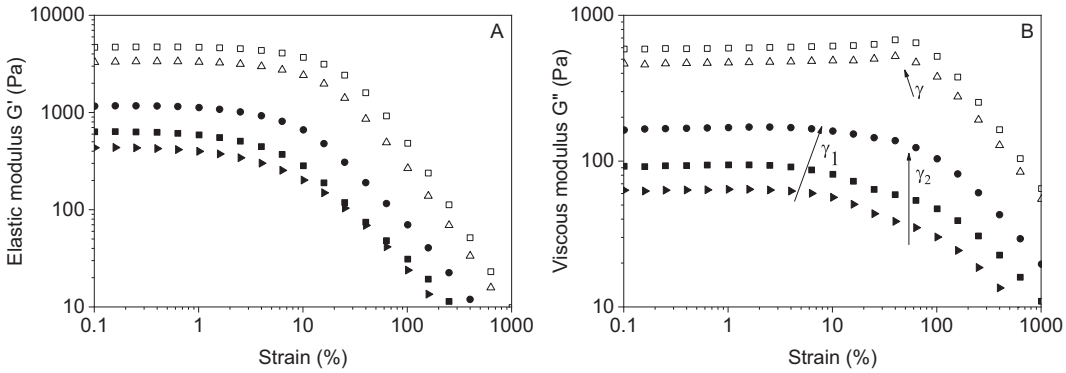

Fig. 2. Elastic modulus, G′, (A) and viscous modulus, G″, (B) as a function of shear strain, γ, for hetero-aggregated emulsions. Oil volume fractions: 0.4 (black triangle), 0.47 (black square), 0.54 (black circle), 0.68 (open triangle), 0.77 (open square). Yielding is indicated in G″ with arrows.

been found for repulsive dispersions (e.g. kaolin) [20] and has also been described for solutions of large (repulsive) polymers, e.g. xanthan [16,21–23]. At very high strains (Fig. 1D), we see that the curve becomes almost squared. Such a shape is normally observed for plastic behaviour [24]. The sharp increase in stress with increasing strain often reflects the elastic deformation of trapped droplets. After a certain strain value, the stress enters a plateau region, indicating that the emulsion starts to flow [25]. Based on these observations, we conclude that the repulsive emulsion shows the behaviour of a soft glassy material.

3.1.2. Attractive emulsions

To vary the attractive interactions among oil droplets, we use different types of interactions; (i) attractive electrostatic interactions, (ii) bridging interactions using a divalent salt (Ca^{2+}) and (iii) cross-linking using polyphenol-protein interactions. The different interaction types and environmental conditions change the strength of the interactions between the emulsion droplets. The effects of these different interactions are discussed separately in the next sections.

3.1.3. Attraction between droplets by electrostatic interactions: Weak interactions

The dependency of the elastic modulus G′ and viscous modulus G″ on shear strain γ for electrostatically attractive emulsions at different oil volume fractions are presented in Fig. 2 and as Lissajous-Bowditch plots in Fig. 3.

G′ increased with increasing oil volume fraction. The absolute values for the elastic modulus were higher for attractive than repulsive interactions at equivalent volume fractions, which can be explained by increased network formation at volume fractions below ϕ_{max} (at $\phi = 0.4$).

For the emulsions with relatively weak interactions, G″ seems to display a two-step yielding in the amplitude sweep (Fig. 2), although this effect is not very prominent. Wall slip as a reason for this yielding behaviour has been excluded by using roughened geometries. The two-step yielding can be seen for a lower volume fraction, $0.4 \leq \phi < 0.6$. The first yield point in G″ occurs around $\gamma \approx 5$-10% and the second at $\gamma \approx 70$–100%. At higher volume fraction of $\phi > 0.7$, the two-step yielding behaviour disappeared. Instead, G″ exhibited a single maximum at a strain γ of ≈60%, close to the strain of the second yield point in the emulsions with $\phi < 0.6$. The possible two-step yielding behaviour suggests that a weak-attractive emulsion undergoes a more complex behaviour than a repulsive emulsion. Such a two-step yielding process in G″ has been reported for other attractive colloidal dispersions, such as polystyrene and gel-particle dispersions [6,7,19,26,27].

The first yielding event, within the weak link regime, is associated with the breaking of weak interactions [6,7,26,27]. The breakage results in rupture of the space-spanning network [27], but emulsion droplets remain clustered. Due to weak attractive interactions, there is constant competition between bond breaking and bond reformation within the cluster. At strain values before the second yielding event takes place, the reformation of bonds to rebuild the network structure and the disruption of the network occur at similar times scales, which delays the event of complete network breakdown. The second yielding is then associated with the breakdown of droplet clusters due to fast structural rearrangements [19,28] and marks the start of material flow.

The first yield point in G″ became less pronounced with increasing ϕ and vanished into a one-step yielding event. We associate this with a decrease in inter-droplet distance with increasing ϕ. The length scales for weak bond breaking (i.e. the first yielding), and caging-related yielding (i.e. the second yielding) come closer to each other [7], and eventually, become equal. Such concentrated emulsions, therefore, mostly exhibit a typical single peak related to cage breakage [29]. Hence, caging of droplets does not only dominate the structural response and mechanical behaviour of repulsive [7] but also of electrostatic, attractive emulsions.

Structural rearrangements were also evaluated in the non-linear regime, by investigating Lissajous-Bowditch plots (Fig. 3A–H) and S- and *T*-factors (Fig. 3I–L). As strain increases, the Lissajous-Bowditch plots show a material response approaching plastic behaviour, indicating that at this point the structure breakdown was advanced. The *T*-factors (Fig. 3I, J), initially increase as a function of strain to about 0.3, suggesting intra-cycle shear thickening, before showing overall shear thinning behaviour. S-factors (Fig. 3K, L) displayed an increasing intra-cycle strain stiffening, reaching values of roughly 1 for emulsions with high volume fractions (0.8). At intermediate volume fractions (0.47) the S-factor (Fig. 3K) showed a local maximum at strains between 10 and 100% before increasing to 1 at higher shear rates. The strain at this maximum coincides with the first yielding of the emulsion. Thus, the response of the S-factor could be a consequence of the first yielding of the emulsion, leading to a local maximum in the S-factor. With increasing strain, the first yielding is overcome, the S-factor drops again before it ultimately increases with further structure breakdown. It should be noted that the strain stiffening for the highest strains in Fig. 3K and 3L is merely an *apparent* strain stiffening. At these strains, as a consequence of the rhomboidal shape of the plots, G_M is approximately zero, and S attains a value of 1. The overall behaviour of the material at these strains is strain softening. This paradox has been extensively discussed in literature [30].

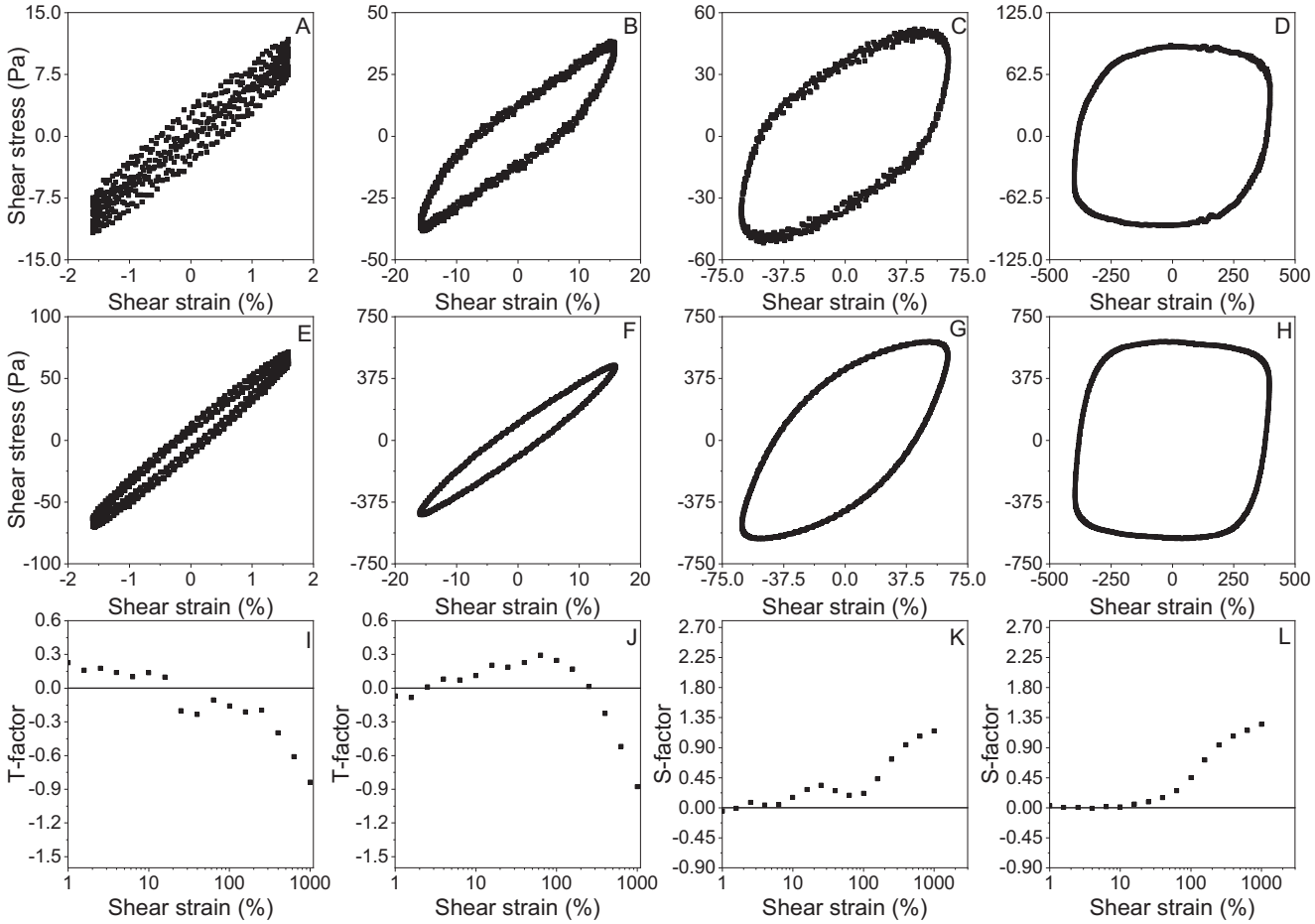

Fig. 3. Overview of LAOS measurements (shear strain vs stress) in 4 strain regions of a weak attractive emulsion (A-D at 0.47 oil) and (E-H at 0.8 oil), the strains in question are: 1.59% (A, E), 15.9% (B, F), 63.4% (C, G) and 400% (D, H). S- and *T*-factors of the emulsion at ϕ = 0.47 (I, K) and ϕ = 0.8 (J, L) are shown as a function of shear strain.

Since the two-step yielding was not obvious, we adjusted the pH of the emulsion, to decrease the interaction strength between the oil droplets and to further investigate this behaviour. By decreasing the pH, we decreased the charge of the emulsifiers on the interface of the droplets, thereby decreasing the interaction strength. The pH was adjusted from 6.3 to 5.5 for the weakly attractive emulsions, with a ϕ of 0.4 and 0.8. The decrease in pH led to a decrease in zeta potential difference, $\Delta\zeta$, between the emulsions from 40 mV at pH 6.3 to 25 mV at pH 5.5. The G′ and G" dependency on shear strain for these emulsions can be found in the supplementary data in Fig. S4.

We observed that G′ decreased due to lower droplet-droplet interaction strength. This difference was evident in the case of ϕ = 0.4, but the effect of interaction strength diminished for a higher volume fraction of 0.8. At higher oil volume fractions, the emulsion is already crowded, and the interactions between the droplets become less relevant. The two-step yielding in the amplitude sweep became less evident. Apparently, for lower droplet-droplet interaction strength the emulsions hardly show resistance to complete cluster disintegration, and thus do not display a clear two-step behaviour. The occurrence of a two-step yielding behaviour was thus not enhanced for lower interaction strength.

3.1.4. Attraction between emulsion droplets by salt-bridges: Intermediate interaction strength

To investigate how stronger interactions affect the rheological behaviour of the dense O/W emulsions, we added a divalent cation (Ca^{2+}) to a protein-stabilised emulsion at a pH at which the protein was negatively charged. The ionic bonds lead to an overall attractive interaction strength and droplet clustering. Figs. 4 and 5 show G′ and G″ as a function of γ and Lissajous-Bowditch plots of emulsions with 0.26 mmol/mL $CaCl_2$ at oil volume fractions of 0.4 and 0.8.

As expected, an increase in G′ was seen for increasing volume fractions. G′ in the linear regime of these emulsions was higher than that of the hetero-aggregated emulsions, confirming a higher interaction strength. At ϕ = 0.4, the moduli displayed an explicit dependency on salt concentration; an increase in salt concentration led to an increase in elastic modulus. For emulsions with an oil volume fraction of 0.8, an increase in salt concentration, however, did not lead to a substantial increase in G′, in line with our findings for hetero-aggregated emulsions. We observe that the extent of the overshoot in G″ is less than in the case of the hetero-aggregated emulsions with weak electrostatic interactions. This indicates that the stronger interactions change the overall flow behaviour of the emulsion from a more soft-glassy to a more gel-like material. In contrast to the emulsions with weak attractive interactions, the two-step yielding is largely reduced. The presence of stronger, and more "inflexible" bonds seemingly decreased the probability of two distinct time scales of yielding and pushed the emulsion towards a more gel-type behaviour [31,32].

In the Lissajous-Bowditch plots, we see that at low strain values, the emulsions show soft glassy behaviour. At intermediate strains, intra-cycle strain-stiffening occurs (Fig. 5G), which suggests that the soft glassy behaviour changed to more gel-like behaviour. Another indication of this transition from soft glassy to gel-like

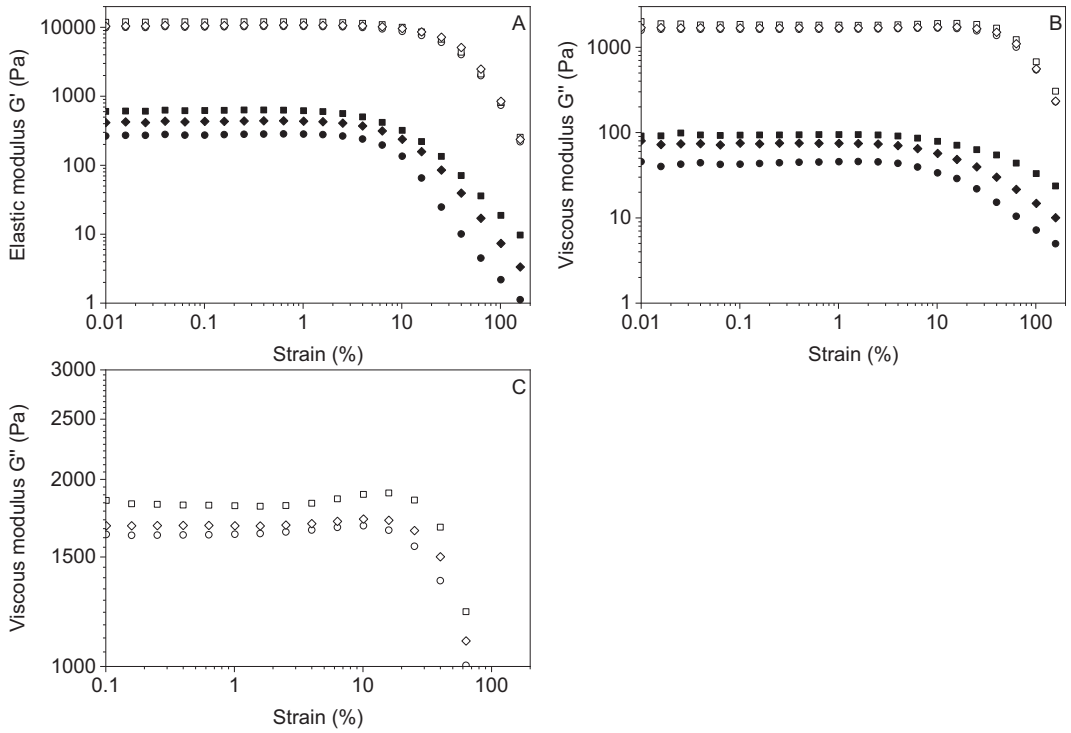

Fig. 4. Elastic modulus, G′, (A) and viscous modulus, G″, (B) as a function of γ for emulsions clustered by salt bridges ($CaCl_2$) at oil volume fractions of 0.4 (open symbols) and 0.8 (filled symbols), differing in salt concentration: 0.03 mmol/mL (circle), 0.13 mmol/mL (diamond), 0.26 mmol/mL (square). A magnification of the yielding area of the viscous modulus, G″, of emulsions with 0.8 vol fraction is shown (C).

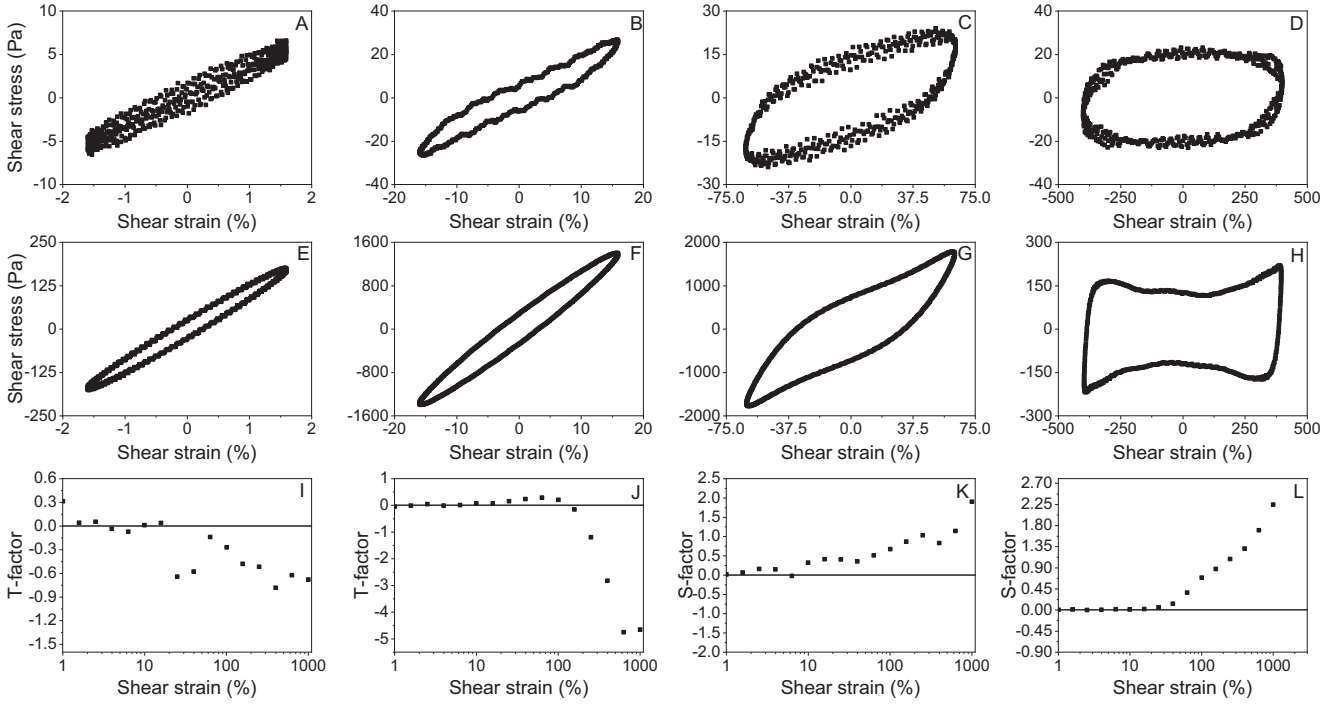

Fig. 5. Overview of LAOS measurements (shear strain vs stress) in 4 strain regions of an attractive emulsion with salt bridges (0.26 mmol/mL $CaCl_2$) (A-D at 0.4 oil) and (E-H at 0.8 oil), the strains in question are: 1.59% (A, E), 15.9% (B, F), 63.4% (C, G) and 400% (D, H). S- and *T*-factors of the emulsion are shown at $\phi = 0.40$ and a salt concentration of 0.26 mmol/mL (I, K), as well as $\phi = 0.8$ and salt: 0.26 mmol/mL (J, L).

behaviour can be seen in the Lissajous-Bowditch plots at high strains (Fig. 5H). The emulsion with $\phi \gg \phi_{max}$ presents a bow-tie shaped curve, which is typically found in gel-like materials [13]. Thus, we conclude that by increasing direct droplet-droplet interactions, the rheological behaviour of the emulsion moved towards that resembling a gel.

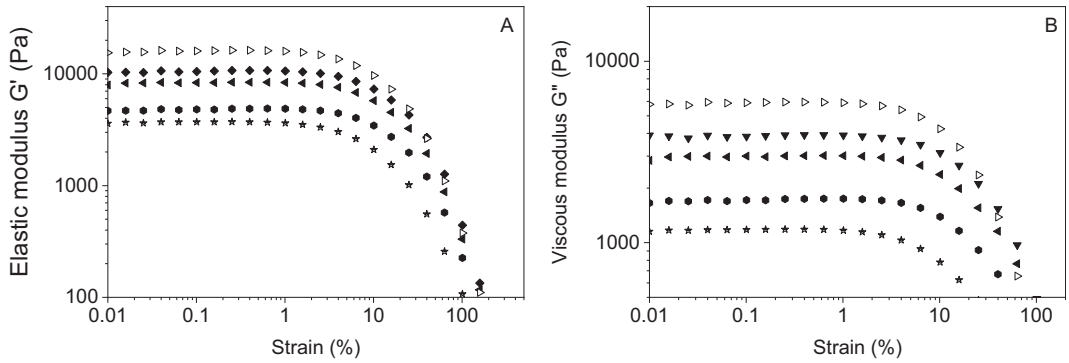

Fig. 6. Elastic modulus, G′, (A) and viscous modulus, G″, (B) as a function of shear strain for protein-stabilised emulsions crosslinked with 0.75% GSE (g/g WPI), with ϕ of 0.4 (downward triangle), 0.47 (diamond), 0.58 (circle), 0.62 (square), 0.85 (triangle).

3.1.5. Attraction between protein-stabilised droplets by polyphenol-protein interactions: Strong interactions

For emulsions with salt bridges, we observed that the rheological behaviour moved towards a more gel-like behaviour. To confirm this transition from soft glassy to gel-like behaviour with increasing interaction strength, we introduced even stronger interactions by crosslinking protein-stabilised droplets by polyphenol-protein interactions. The results obtained from the oscillatory strain sweep are presented in Fig. 6 and Lissajous-Bowditch plots in Fig. 7.

The higher values of G′ and G″ confirm that indeed stronger interactions are present. This is the result of a combination of different interaction types [33]. Interestingly, the dependency of G′ and G″ on ϕ was less pronounced for the emulsions with strongly interacting droplets, compared to that of electrostatically attractive emulsions or emulsions containing divalent salts. This suggests that the strong inter-droplet interactions create a strong space-spanning network already at low oil volume fractions and an increase in volume fraction only has a small additional contribution to the emulsion elasticity. Furthermore, emulsions with strongly interacting droplets did not show a G″ overshoot above ϕ_{max} or in the *T*-factor, in contrast to the emulsions with weaker interactions (electrostatic or salt-bridging). This implies gel-like behaviour. A further indication of the transition towards gel-like behaviour can be seen from the Lissajous-Bowditch plots. In Fig. 7 C and G, the Lissajous-Bowditch plots for the emulsions with strong attractive interactions showed an upward convex nature indicating intra-cycle stiffening (as also shown by the S-factors) after intra-cycle strain-softening. A similar interpretation of the upward convex nature of Lissajous plots has been provided earlier [22]. Even though Lissajous-Bowditch plots at high strains (Fig. 7D and H) have to be examined with care, as the occurrence of wall slip phenomena cannot be completely excluded, the change in the shape of Lissajous-Bowditch curves show similarities with the upward edges observed by Zhang and co-workers in 2D for silica particle-laden interfaces, [9], and in 3D by Precha-Atsawanan and co-workers in starch gels [13]. This behaviour is typically observed for samples that exhibit a gel-like behaviour and a monotonous decrease in G″ when plotted against the strain. The abrupt yielding behaviour in the amplitude sweeps and the fast decrease in moduli has been attributed to high bond energy among the droplets [31]. The high bonding energy makes breakage of bonds and the occurrence of distinct yielding phenomena difficult. At both $\phi < \phi_{max}$ and $\phi > \phi_{max}$, the yielding in G″ ($\gamma \approx 10\%$) can be assumed to result from network disintegration rather than a step-wise breakage of droplet clusters and cluster–cluster interactions, as has been discussed by others [19,26,27].

3.1.6. Effect of interaction strength on rheological behaviour

Previous research suggested that attractive interactions lead to a two-step yielding behaviour of colloidal glasses due to the occurrence of two distinct relaxation phenomena [6,7,19]. This raises the question of why such behaviour only occurred for emulsions with weaker attractive interactions, and not for those with stronger ones.

In studies that reported a two-step yielding behaviour, particle or droplet interactions were mostly induced by depletion interactions or by screening of repulsive interactions [6,9,19]. Depletion interactions, however, are the result of an exclusion process rather than of direct attraction among particles. Therefore, the interaction strength among droplets is weak, reversible, and flexible [34]. In contrast, the interactions investigated in this study were direct attractive droplet-droplet interactions, and, therefore, significantly stronger. Thus, they resulted in the formation of less flexible bonds. This suggests that a two-step yielding behaviour in emulsions can not only occur in a limited volume fraction range but also within a limited interaction strength range.

Interaction strength among droplets also affects the rheology of emulsions at $\phi > \phi_{max}$. For concentrated emulsions with repulsive and weak attractive interactions, we observed an overshoot in G″ and apparent strain-hardening in the amplitude sweep and the *T*-factors, linked to temporary densification of the droplets before the emulsion started to flow. Thus, weakly attractive emulsions behave at $\phi > \phi_{max}$ as soft glasses. Concentrated emulsions with strongly attractive interactions at $\phi > \phi_{max}$, did not show this overshoot. The monotonous strain-softening behaviour in the amplitude sweep also occurs in gels, where orientation and alignment of the microstructure cause strain softening [35]. The presence of strong and inflexible bonds among droplets decreases the probability of network rupture and structural rearrangements of bonds. In emulsions with strong interactions, inter-cluster rearrangements are more likely to occur than intra-cluster rearrangements. It appears that droplet clusters do not disintegrate, but rather align along the flow direction, causing shear thinning behaviour [34]. Intra-cluster rearrangements refer in this context to rearrangements of individual droplets within a cluster, whereas inter-cluster rearrangements refer to rearrangements between clusters, rather than between droplets [26,27]. Thus, at high volume fractions, emulsions with strong, attractive interactions behave as gels.

3.2. Volume fraction dependencies

To compare emulsions with weak attractive, strong attractive and repulsive interactions, relevant rheological parameters of the studied emulsions were plotted as a function of ϕ (Fig. 8).

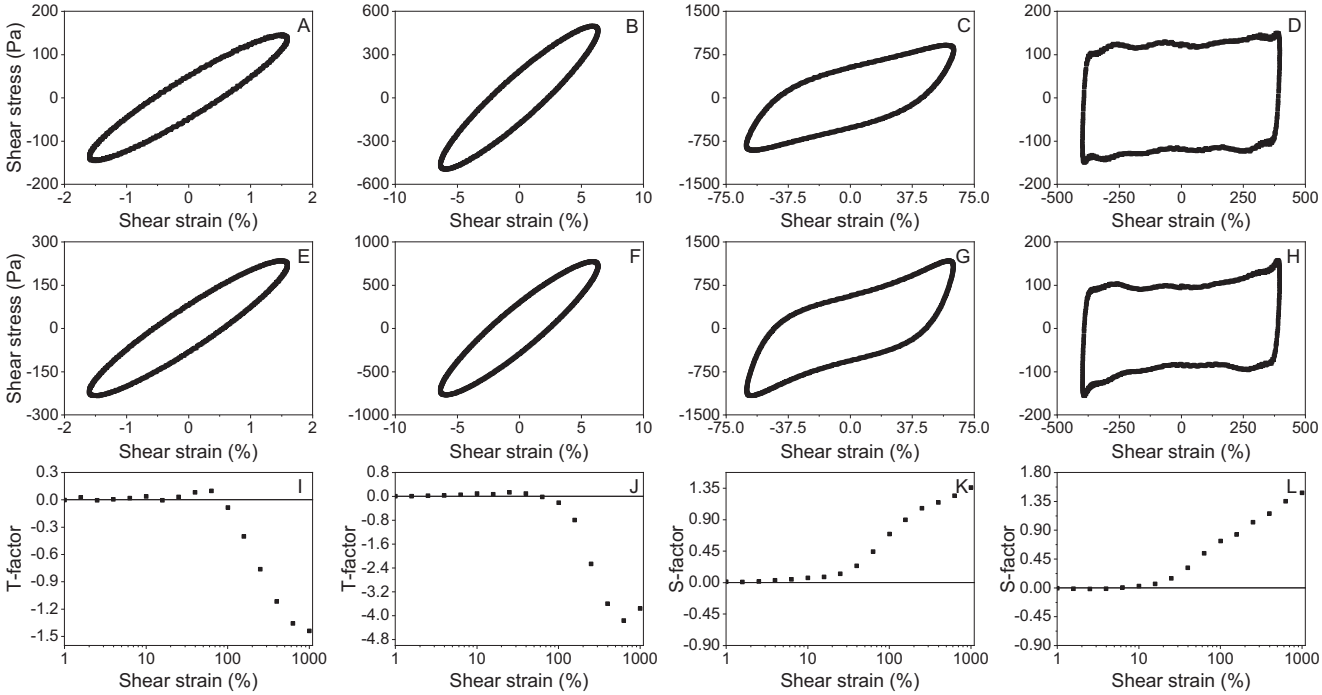

Fig. 7. Overview of LAOS measurements (shear strain vs stress) in 4 strain regions of an attractive emulsion with strong attractive interactions (A-D at 0.47 oil) and (E-H at 0.8 oil), the strains in question are: 1.59% (A, E), 15.9% (B, F), 63.4% (C, G) and 400% (D, H). S- and *T*-factors of the emulsion at ϕ = 0.47 (I, K) and ϕ = 0.8 (J, L) are shown as a function of shear strain.

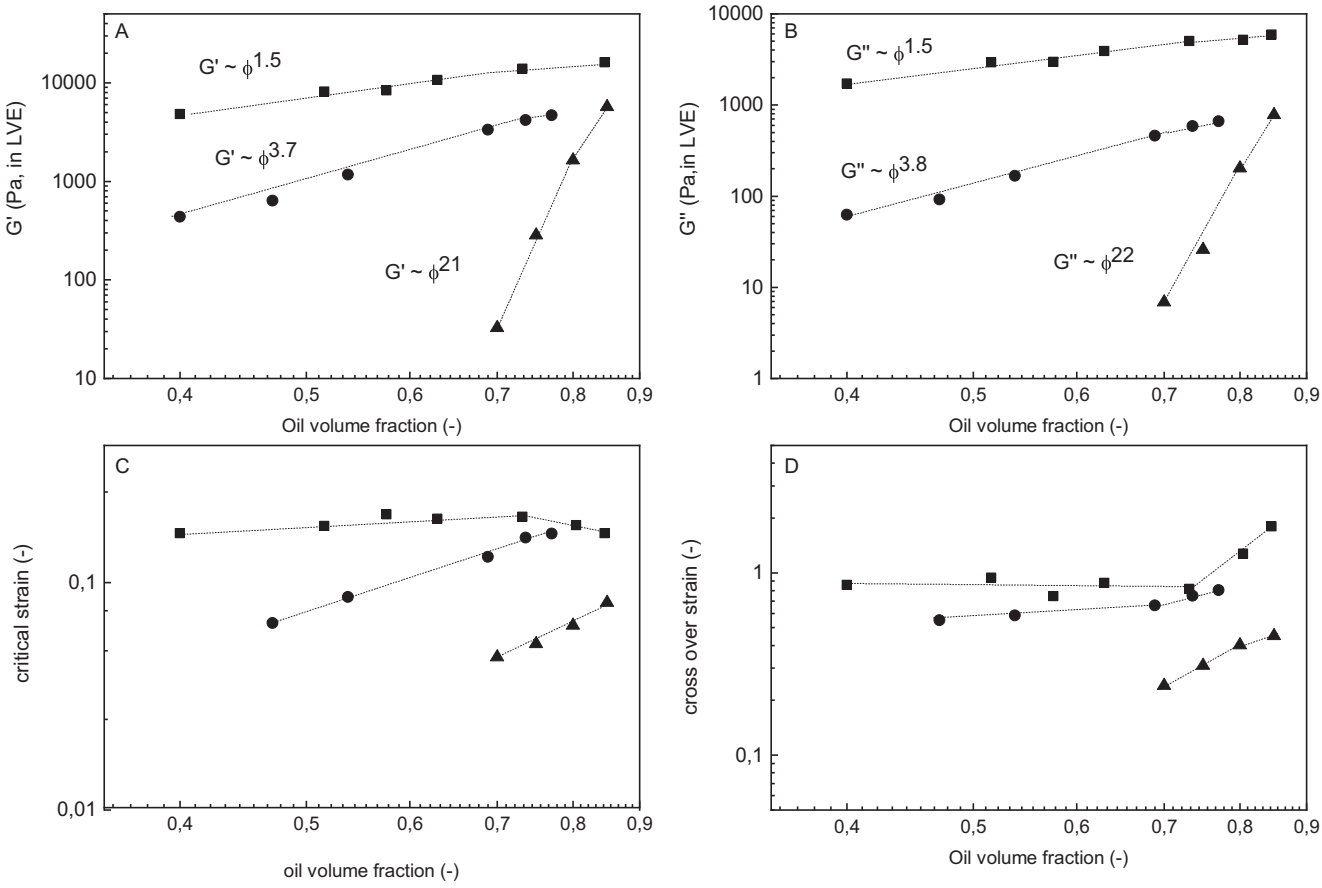

Fig. 8. Elastic modulus, G′, (A) and viscous modulus, G″, (B) (at γ = 0.1%), cross-over strain (D), critical/yield strain (C) as a function of oil ϕ for emulsions crosslinked by GSE (squares), hetero-aggregated emulsions (circles) and repulsive emulsions (triangles). The lines are added to guide the eye. Indications of the power-law index n of $G' \sim \phi^n$ and $G'' \sim \phi^n$ are provided (data was fitted until $\phi < \phi max$, all samples R2 > 0.98).

3.2.1. Modulus dependency on the volume fraction

The values for G′ were lowest for the repulsive emulsions and highest for the strong attractive emulsions. For emulsions with attractive interactions, also a lower power-law dependence of G′ and G″ with volume fraction was observed. This power-law dependence became weaker with increases in cluster strength. This observation supports the assumed differences in interaction strength between droplets, in line with literature. Stieger et al. showed for colloidal microgels that the slope of G, as a function of the effective volume fraction, depends on the interaction potential [37]. Thus, from a mechanistic perspective, the lower power-law dependency of the moduli on oil volume fraction indicates strong network formation and gel-like behaviour. Repulsive and weak attractive emulsions, behaving as glassy materials, have a much stronger dependency on volume fraction, which was also reported earlier for suspensions of poly-methylmethacrylate (PMMA) particles and in theoretical work [7,38,39].

3.2.2. Yield strain dependency on the volume fraction

The interactions between the droplets also affect the yielding behaviour of the emulsions. In our study, emulsions with strong attractive interactions exhibited the highest yield (critical) strain values, whereas the lowest values were found for repulsive emulsions (Fig. 8C). This is consistent with results reported for hard-sphere dispersions [40–42]. All emulsions showed an increase in critical strain with increasing ϕ. However, for strongly attractive interactions (cross-linked by polyphenols, GSE), this increase was only visible up to a volume fraction of roughly 0.7, after which the critical strain slightly decreased when volume fraction increased even further. The decrease in critical strain upon approaching close packing indicates that these strongly flocculated samples become more brittle [7]. This might be caused by a reduction in deformability of clusters when inter-droplet interactions are strong [43], and increased the rigidity of the gel [44].

3.2.3. Cross-over point dependency on the volume fraction

The cross-over strain (Fig. 8D) at a given ϕ was higher for the attractive emulsions than for the repulsive emulsion, with the strongly flocculated emulsion (polyphenols, GSE) exhibiting highest values over the ϕ range. This indicates that the solid–liquid transition shifts to higher γ with increasing strength of attractive inter-droplet interactions. Structural rearrangement leading to flow is less easily achieved due to strong interactions.

3.3. Glass or gel?

Attractive emulsions differ in their rheological response not only from repulsive emulsions, but also significant differences were observed between them. The rheology of such materials depends on ϕ and the inter-droplet interaction strength, but also whether interactions are non-specific, such as depletion interactions, or specific interactions, such as in case of the attractive emulsions, based on electrostatic droplet-droplet interactions or droplet-droplet cross-linking. Non-specific weak interactions, such as depletion interactions [19], and weak attractive interactions (shown in this study) show a two-step yielding phenomenon, while this phenomenon disappears for stronger interactions This indicates that different classes of viscoelastic solids can be obtained, and normally a distinction between glassy materials and gels are made. In the case of our attractive emulsions at high ϕ, structure breakdown likely occurs due to intra-cluster and inter-cluster rearrangements, as well as caging effects. These events depend on the interactions within and between clusters and therefore contribute to the emulsion microstructure and rheological response. Such behaviour is quite diverse, and the classification of glasses and gels is not sufficient to describe these differences. Previously, it was already discussed that glasses can be subdivided into repulsive and attractive glasses [45]. The results of this study suggest that further differentiation among attractive

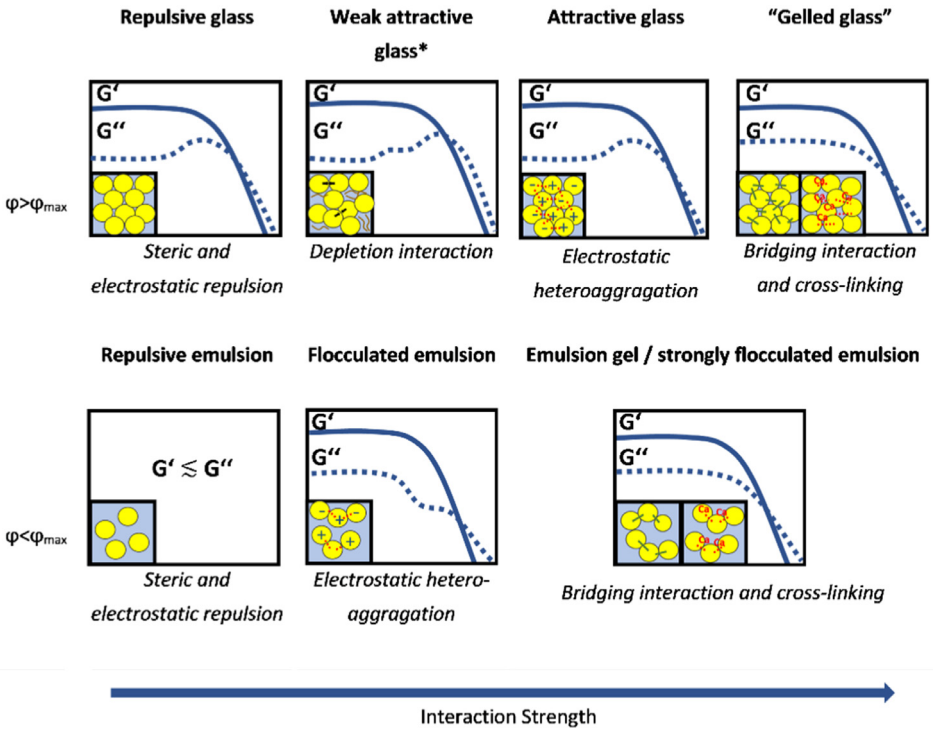

Fig. 9. Classification of emulsions depending on volume fraction and interaction strength/type. The corresponding schematic representation of G′ (line) and G″ (dashed line) dependency during strain-controlled LAOS measurements is shown. A characteristic behaviour of G′/G″ (ϕ < ϕmax) for sterically/electrostatically stabilised emulsions is not shown, as measured moduli are typically very low and measured torques are close to lower torque limits. For those materials G′ is typically < G″. The behaviours shown in the classification tend to transition from one to another.

emulsions might also be more appropriate. A graphical representation of our suggestion for such differentiation can be also found in Fig. 9. At $\phi > \phi_{max}$, emulsions are generally in a glassy state. However, an increase in (attractive) interaction strength can shift a glassy state to a gelled state, as also previously proposed [15]. This shift also changes the yielding behaviour, from a tendency to show multiple yielding events to a monotonous yielding. We can, therefore, differentiate between repulsive, weak attractive, attractive, and "gelled" emulsions, depending on interaction type/strength.

4. Conclusion

We hypothesised that the rheological response and yielding of emulsions are influenced by the type of droplet-droplet interactions and interaction strength and that the behaviour can be mapped using small (SAOS) and large (LAOS) amplitude oscillatory shear measurements. Through characterisation of emulsions with a broad range of interaction strengths, this work extends earlier research and adds to existing literature by showing that specific yielding phenomena, such as two-step yielding, are not ubiquitous but strongly depend on the interaction between the dispersed droplets [7,41,46].

Our findings show that dominant factors in emulsion rheology are droplet interaction strength as a function of droplet volume fraction. Strong interactions lead to gel-like behaviour, while weak interactions lead to soft glassy behaviour and two-step yielding. At $\phi > \phi_{max}$, caging effects become more relevant for the elastic modulus of a material, partially overruling effects of droplet interactions, as seen by the weakening of the dependency of the elastic modulus on droplet-droplet interactions at $\phi > \phi_{max}$. The experimental results suggest that a further differentiation among attractive emulsions is appropriate. Based on this evidence, we propose to extend current classifications of emulsions [45], by differentiating between repulsive, weak attractive, attractive, and "gelled" emulsions, depending on interaction strength. The transitions between the different systems seem to be gradual. The insights provided in this research help to identify the microstructure of emulsions through rheological fingerprinting, but also allows to extend the performance of materials through controlled changes in composition to affect the overall droplet interactions. Future work can include the investigation of the role of droplet deformability and microscopy techniques to clarify the mechanisms of the two-step yielding process.

5. Financial disclosure

The project is organised by and executed under the auspices of TiFN, a public–private partnership on precompetitive research in food and nutrition. Funding for this research was obtained from FrieslandCampina, Fromageries Bel, and Unilever, the Netherlands Organisation for Scientific Research, and the Top-sector Agri&Food.

CRediT authorship contribution statement

Philipp L. Fuhrmann: Conceptualization, Methodology, Formal analysis, Writing – original draft. **Swantje Breunig:** Investigation, Visualization. **Guido Sala:** Writing – review & editing, Supervision. **Leonard Sagis:** Writing – review & editing, Supervision. **Markus Stieger:** Writing – review & editing, Supervision, Project administration, Funding acquisition. **Elke Scholten:** Writing – review & editing, Supervision.

Declaration of Competing Interest

The authors declare that they have no known competing financial interests or personal relationships that could have appeared to influence the work reported in this paper.

Appendix A. Supplementary material

Supplementary data to this article can be found online at https://doi.org/10.1016/j.jcis.2021.08.124.

References

[1] E. Dickinson, Colloids in Food: Ingredients, Structure, and Stability, Annu. Rev. Food Sci. Technol. 6 (1) (2015) 211–233, https://doi.org/10.1146/annurev-food-022814-015651.
[2] P. Fischer, E.J. Windhab, Rheology of food materials, Curr. Opin. Colloid Interface Sci. 16 (1) (2011) 36–40, https://doi.org/10.1016/j.cocis.2010.07.003.
[3] M. Hermes, P.S. Clegg, Yielding and flow of concentrated Pickering emulsions, Soft Matter. 9 (2013) 7568–7575, https://doi.org/10.1039/C3SM50889G.
[4] O. Mondain-Monval, F. Leal-Calderon, J. Phillip, J. Bibette, Depletion forces in the presence of electrostatic double layer repulsion, Phys. Rev. Lett. 75 (18) (1995) 3364–3367, https://doi.org/10.1103/PhysRevLett.75.3364.
[5] V.V. Erramreddy, S. Ghosh, Influence of droplet size on repulsive and attractive nanoemulsion gelation, Colloids Surf. Physicochem. Eng. Asp. 484 (2015) 144–152, https://doi.org/10.1016/j.colsurfa.2015.07.027.
[6] S.S. Datta, D.D. Gerrard, T.S. Rhodes, T.G. Mason, D.A. Weitz, Rheology of attractive emulsions, Phys. Rev. E. 84 (2011) 41404, https://doi.org/10.1103/PhysRevE.84.041404.
[7] N. Koumakis, G. Petekidis, Two step yielding in attractive colloids: transition from gels to attractive glasses, Soft Matter 7 (2011) 2456–2470, https://doi.org/10.1039/C0SM00957A.
[8] P.L. Fuhrmann, G. Sala, M. Stieger, E. Scholten, Clustering of oil droplets in o/w emulsions: controlling cluster size and interaction strength, Food Res. Int. 122 (2019) 537–547, https://doi.org/10.1016/j.foodres.2019.04.027.
[9] H. Zhang, K. Yu, O.J. Cayre, D. Harbottle, Interfacial particle dynamics: one and two step yielding in colloidal glass, Langumir 32 (50) (2016) 13472–13481, https://doi.org/10.1021/acs.langmuir.6b0358610.1021/acs.langmuir.6b03586.s001.
[10] Z. Zhou, J.V. Hollingsworth, S. Hong, H.e. Cheng, C.C. Han, Yielding behavior in colloidal glasses: comparison between "hard cage" and "soft cage", Langmuir 30 (20) (2014) 5739–5746, https://doi.org/10.1021/la500866d.
[11] C. Christopoulou, G. Petekidis, B. Erwin, M. Cloitre, D. Vlassopoulos, Ageing and yield behaviour in model soft colloidal glasses, Philos. Trans. R. Soc. Math. Phys. Eng. Sci. 367 (2009) 5051–5071, https://doi.org/10.1098/rsta.2009.0166.
[12] R.H. Ewoldt, A.E. Hosoi, G.H. Mckinley, Rheological fingerprinting of complex fluids using large amplitude oscillatory shear (LAOS) flow, Annu. Trans.-Nord. Rheol. Soc. 15 (2007) 3.
[13] S. Precha-Atsawanan, D. Uttapap, L.M.C. Sagis, Linear and nonlinear rheological behavior of native and debranched waxy rice starch gels, Food Hydrocoll. 85 (2018) 1–9, https://doi.org/10.1016/j.foodhyd.2018.06.050.
[14] G. Giménez-Ribes, M. Habibi, L.M.C. Sagis, Interfacial rheology and relaxation behavior of adsorption layers of the triterpenoid saponin Escin, J. Colloid Interface Sci. 563 (2020) 281–290, https://doi.org/10.1016/j.jcis.2019.12.053.
[15] H. Tanaka, J. Meunier, D. Bonn, Nonergodic states of charged colloidal suspensions: Repulsive and attractive glasses and gels, Phys. Rev. E - Stat. Stat. Nonlinear Soft Matter Phys. 69 (3) (2004), https://doi.org/10.1103/PhysRevE.69.031404.
[16] K. Hyun, S.H. Kim, K.H. Ahn, S.J. Lee, Large amplitude oscillatory shear as a way to classify the complex fluids, J. Non-Newton. Fluid Mech. 107 (1-3) (2002) 51–65, https://doi.org/10.1016/S0377-0257(02)00141-6.
[17] T.G. Mezger, The Rheology Handbook, 2009. https://doi.org/10.1108/prt.2009.12938eac.006.
[18] H.S. Kim, T.G. Mason, Advances and challenges in the rheology of concentrated emulsions and nanoemulsions, Adv. Colloid Interface Sci. 247 (2017) 397–412, https://doi.org/10.1016/j.cis.2017.07.002.
[19] K.N. Pham, G. Petekidis, D. Vlassopoulos, S.U. Egelhaaf, W.C.K. Poon, P.N. Pusey, Yielding behavior of repulsion- and attraction-dominated colloidal glasses, J. Rheol. 52 (2) (2008) 649–676, https://doi.org/10.1122/1.2838255.
[20] F. Bossard, M. Moan, T. Aubry, Linear and nonlinear viscoelastic behavior of very concentrated plate-like kaolin suspensions, J. Rheol. 51 (6) (2007) 1253–1270, https://doi.org/10.1122/1.2790023.
[21] M.E. Helgeson, Y. Gao, S.E. Moran, J. Lee, M. Godfrin, A. Tripathi, A. Bose, P.S. Doyle, Homogeneous percolation versus arrested phase separation in attractively-driven nanoemulsion colloidal gels, Soft Matter 10 (2014) 3122–3133, https://doi.org/10.1039/c3sm52951g.
[22] J. John, D. Ray, V.K. Aswal, A.P. Deshpande, S. Varughese, Dissipation and strain-stiffening behavior of pectin-Ca gels under LAOS, Soft Matter 15 (34) (2019) 6852–6866, https://doi.org/10.1039/C9SM00709A.

[23] T.G. Mason, J. Bibette, D.A. Weitz, Elasticity of compressed emulsions, Phys. Rev. Lett. 75 (10) (1995) 2051–2054, https://doi.org/10.1103/PhysRevLett.75.2051.
[24] R.H. Ewoldt, P. Winter, J. Maxey, G.H. Mckinley, R.H. Ewoldt, P. Winter, G.H. Mckinley, J. Maxey, Large amplitude oscillatory shear of pseudoplastic and elastoviscoplastic materials, Rheol. Acta 49 (2010) 191–212, https://doi.org/10.1007/s00397-009-0403-7.
[25] R. Shu, W. Sun, T. Wang, C. Wang, X. Liu, Z. Tong, Linear and nonlinear viscoelasticity of water-in-oil emulsions: Effect of droplet elasticity, Colloids Surf. Physicochem. Eng. Asp. 434 (2013) 220–228, https://doi.org/10.1016/j.colsurfa.2013.05.057.
[26] M. Laurati, S.U. Egelhaaf, G. Petekidis, Plastic rearrangements in colloidal gels investigated by LAOS and LS-Echo, Cit. J. Rheol. 58 (5) (2014) 1395–1417, https://doi.org/10.1122/1.4872059.
[27] M. Laurati, S.U. Egelhaaf, G. Petekidis, Nonlinear rheology of colloidal gels with intermediate volume fraction, J. Rheol. 55 (3) (2011) 673–706, https://doi.org/10.1122/1.3571554.
[28] M. Parthasarathy, D.J. Klingenberg, Large amplitude oscillatory shear of ER suspensions, J. Non-Newton. Fluid Mech. 81 (1-2) (1999) 83–104, https://doi.org/10.1016/S0377-0257(98)00096-2.
[29] K. van der Vaart, Y. Rahmani, R. Zargar, Z. Hu, D. Bonn, P. Schall, Rheology of concentrated soft and hard-sphere suspensions, J. Rheol. 57 (4) (2013) 1195–1209, https://doi.org/10.1122/1.4808054.
[30] M.R.B. Mermet-Guyennet, J. Gianfelice de Castro, M. Habibi, N. Martzel, M.M. Denn, D. Bonn, LAOS: The strain softening/strain hardening paradox, J. Rheol. 59 (1) (2015) 21–32, https://doi.org/10.1122/1.4902000.
[31] J. Appel, B. Fölker, J. Sprakel, Mechanics at the glass-to-gel transition of thermoresponsive microgel suspensions, Soft Matter. 12 (9) (2016) 2515–2522, https://doi.org/10.1039/C5SM02940F.
[32] T.B.J. Blijdenstein, W.P.G. Hendriks, E. van der Linden, T. van Vliet, G.A. van Aken, Control of Strength and Stability of Emulsion Gels by a Combination of Long-and Short-Range, Interactions 19 (17) (2003) 6657–6663, https://doi.org/10.1021/la0342969.
[33] M.C. Bohin, J.P. Vincken, A.H. Westphal, A.M. Tripp, P. Dekker, H.T. van der Hijden, H. Gruppen, Interaction of flavan-3-ol derivatives and different caseins is determined by more than proline content and number of proline repeats, Food Chem. 158 (2014) 408–416, https://doi.org/10.1016/j.foodchem.2014.02.145.
[34] T.B.J. Blijdenstein, A.J.M.V. Winden, T.V. Vliet, E.V.D. Linden, G.A. van Aken, Serum separation and structure of depletion- and bridging-flocculated emulsions: A comparison, Colloids Surf. Physicochem. Eng. Asp. 245 (1-3) (2004) 41–48, https://doi.org/10.1016/j.colsurfa.2004.07.002.
[35] H.G. Sim, K.H. Ahn, S.J. Lee, Large amplitude oscillatory shear behavior of complex fluids investigated by a network model: A guideline for classification, J. Non-Newton. Fluid Mech. 112 (2-3) (2003) 237–250, https://doi.org/10.1016/S0377-0257(03)00102-2.
[36] S.H. Kim, H.G. Sim, K.H. Ahn, S.J. Lee, Large amplitude oscillatory shear behavior of the network model for associating polymeric systems, Korea-Aust. Rheol. J. 14 (2002) 49–55.
[37] M. Stieger, W. Richtering, J.S. Pedersen, P. Lindner, Small-angle neutron scattering study of structural changes in temperature sensitive microgel colloids, J. Chem. Phys. 120 (13) (2004) 6197–6206, https://doi.org/10.1063/1.1665752.
[38] N. Koumakis, A.B. Schofield, G. Petekidis, Effects of shear induced crystallization on the rheology and ageing of hard sphere glasses, Soft Matter. 4 (2008) 2008–2018, https://doi.org/10.1039/B805171B.
[39] H. Lowen, Elastic constants of the hard-sphere glass: a density functional approach, J. Phys. Condens. Matter. 2 (42) (1990) 8477–8484, https://doi.org/10.1088/0953-8984/2/42/024.
[40] N. Selway, J.R. Stokes, Soft materials deformation, flow, and lubrication between compliant substrates: impact on flow behavior, mouthfeel, stability, and flavor, Annu. Rev. Food Sci. Technol. 5 (1) (2014) 373–393, https://doi.org/10.1146/annurev-food-030212-182657.
[41] M. Priya, T.h. Voigtmann, Nonlinear rheology of dense colloidal systems with short-ranged attraction: a mode-coupling theory analysis, J. Rheol. 58 (5) (2014) 1163–1187, https://doi.org/10.1122/1.4871474.
[42] Y. Zong, G. Yuan, C. Zhao, C.C. Han, Differentiating bonding and caging in a charged colloid system through rheological measurements, J. Chem. Phys. 138 (18) (2013) 184902, https://doi.org/10.1063/1.4803857.
[43] A. Montesi, A.A. Peña, M. Pasquali, Vorticity alignment and negative normal stresses in sheared attractive emulsions, Phys. Rev. Lett. 92 (2004) 58303, https://doi.org/10.1103/PhysRevLett.92.058303.
[44] E. Dickinson, Emulsion gels: The structuring of soft solids with protein-stabilized oil droplets, Food Hydrocoll. 28 (1) (2012) 224–241, https://doi.org/10.1016/j.foodhyd.2011.12.017.
[45] L. Cipelletti, L. Ramos, Slow dynamics in glasses, gels and foams, Curr. Opin. Colloid Interface Sci. 7 (3-4) (2002) 228–234, https://doi.org/10.1016/S1359-0294(02)00051-1.
[46] D.B. Genovese, J.E. Lozano, M.A. Rao, The rheology of colloidal and noncolloidal food dispersions, J. Food Sci. 72 (2) (2007) R11–R20, https://doi.org/10.1111/jfds.2007.72.issue-210.1111/j.1750-3841.2006.00253.x.